LA-3734

LOS ALAMOS SCIENTIFIC LABORATORY
of the
University of California
LOS ALAMOS • NEW MEXICO

Transfer Functions for Circulating-Fuel Reactors

UNITED STATES
ATOMIC ENERGY COMMISSION
CONTRACT W-7405-ENG. 36

DISCLAIMER

This report expresses the opinions of the author or authors and does not necessarily reflect the opinions or views of the Los Alamos Scientific Laboratory.

Printed in the United States of America. Available from
Clearinghouse for Federal Scientific and Technical Information
National Bureau of Standards, U. S. Department of Commerce
Springfield, Virginia 22151
Price: Printed Copy $3.00; Microfiche $0.65

LA-3734
UC-80, REACTOR TECHNOLOGY
TID-4500

LOS ALAMOS SCIENTIFIC LABORATORY
of the
University of California
LOS ALAMOS • NEW MEXICO

Report written: May 1967

Report distributed: September 21, 1967

Transfer Functions for Circulating-Fuel Reactors

by

B. J. Henderson

G. L. Ragan

THIS PAGE

WAS INTENTIONALLY

LEFT BLANK

TRANSFER FUNCTIONS FOR CIRCULATING-FUEL REACTORS

by

B. J. Henderson and G. L. Ragan

ABSTRACT

The zero-power transfer function, the power feedback transfer function, and the total reactor transfer function have been determined analytically for a direct-contact, circulating-fuel reactor. Decay and extraction of delayed neutron precursors in the loop outside the core, and the variation of the coolant temperature in this loop are considered. A FORTRAN-II program has been coded for the IBM 704, and graphs present the results of some parametric studies. The analytic expressions are applicable to circulating-fuel reactors in general, but the parameter values used in the studies reported here are based on conceptual direct-contact reactor designs.

INTRODUCTION

Control analysis of a direct-contact, circulating-fuel reactor system[1] must include, in addition to the usual temperature feedback effects, the reactivity effects associated with delayed neutron precursors leaving and re-entering the core. These reactivity effects are complicated by the partial extraction of the delayed neutron precursors[2] in the external loop in addition to their decay in this loop. Analysis should show whether or not resonances occur in the frequency response of this system and also whether or not self-sustained power oscillations result.

In this report, analytical expressions are developed separately for the zero-power transfer function and for the power feedback transfer function; they are then combined to form the total reactor transfer function. The zero-power transfer function is determined from a modified form of the reactor kinetic equations. The power feedback transfer function results from solution of the heat balance equations for the core, heat exchanger, and circulating loop.

This study is similar to that of MacPhee,[3] but it is extended to include partial extraction of delayed neutron precursors, six groups of delayed neutrons, and operation at nonzero power. Numerical values of transfer functions are obtained, by use of a FORTRAN-II program, over a wide range of frequencies. The code permits easy variation of the neutron times in the core and in the loop, degree of extraction of precursors in the external loop, and power levels.

Throughout this study, certain arbitrary simplifying assumptions are made, the validity of each varying from one reactor design to another. The assumptions* are as follows:

i) Reactor kinetic equations are spatially independent.

ii) No fissions occur outside the core.

iii) Both fuel and coolant flows are constant.

iv) The fuel entering the core is instantly mixed with the fuel already there, and the fuel leaving it has the temperature and precursor concentration of the core mixture.

---

* The first five assumptions are equivalent to those of MacPhee, and they are believed to be reasonable for the geometries shown in Figs. 1 and 2. In Fig. 2, droplets of fuel leaving the core through holes around the bottom are intimately mixed into the coolant stream flowing upward around the core. After separation from the coolant, the fuel collects in a pool and returns to the core.

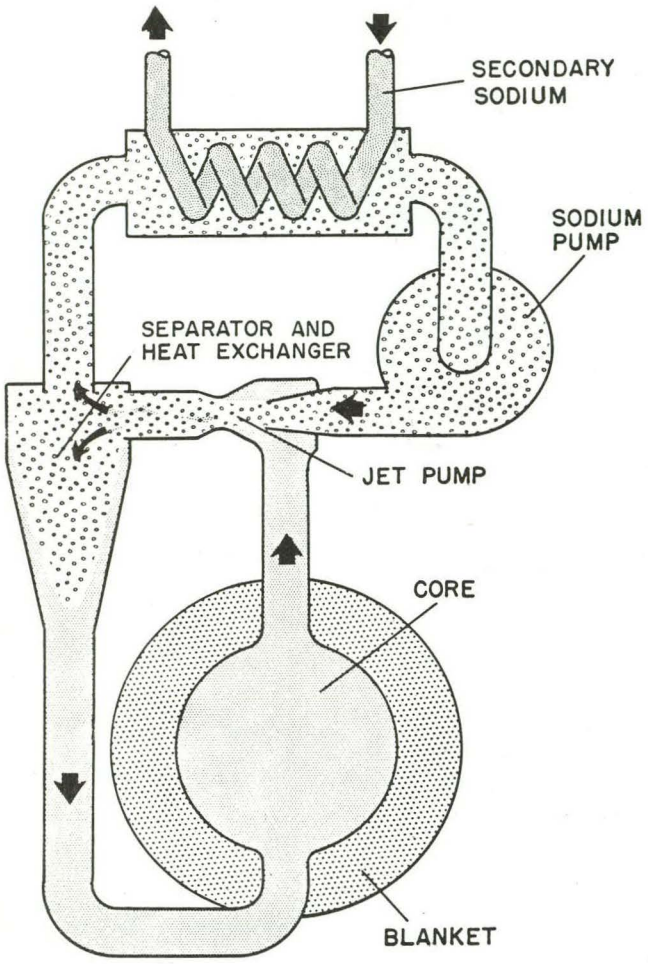

Fig. 1. Schematic drawing of a direct-contact reactor core.

v) The fuel flows in slug flow in the circuit outside the core.

vi) Isothermal* conditions exist separately in each of the three fuel regions of Fig. 3: core, heat exchanger, and return.

vii) The temperature of the sodium coolant entering the heat exchanger is constant. Within the heat exchanger, the coolant is isothermal.

ZERO-POWER TRANSFER FUNCTION

The zero-power transfer function is determined from a modified version of the reactor kinetic equations. These equations include terms representing the loss of neutron precursors in the external loop due to both decay and extraction. A schematic drawing and a preliminary proposal for a direct-contact, circulating-fuel reactor are shown in Figs. 1 and 2. The corresponding model used in the present study is given in Fig. 3 with nomenclature as follows:

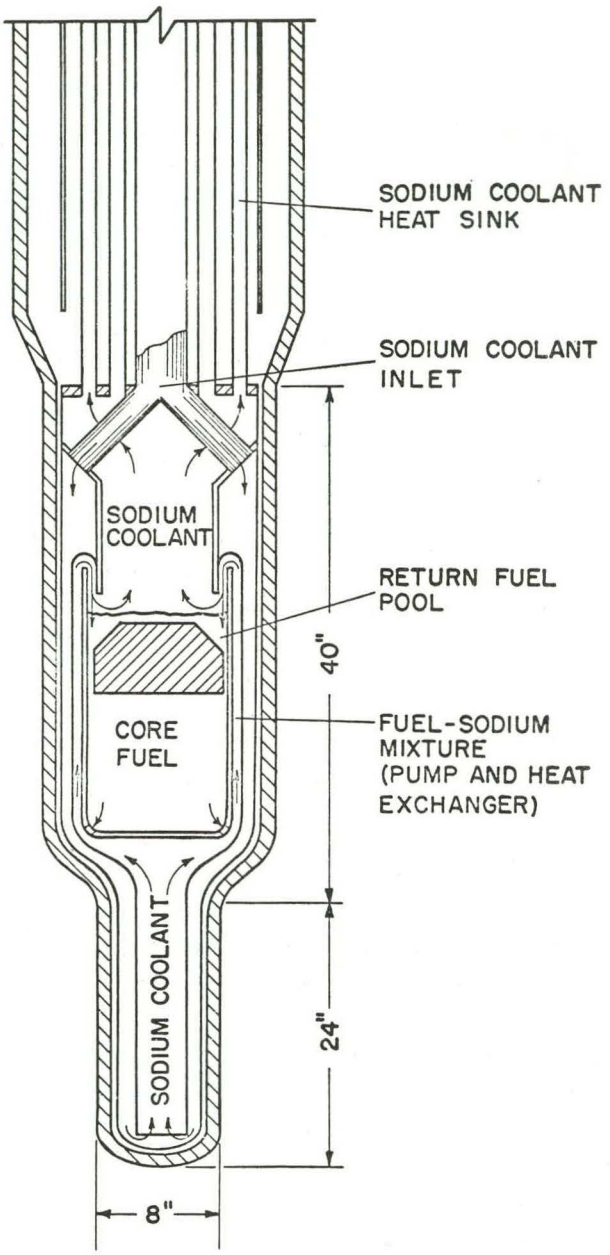

Fig. 2. Proposed 15-MW core for Fast Reactor Core Test Facility.

V_c = volume of fuel in core

V_ℓ = volume of fuel in external loop

F = volumetric flow rate of fuel

* Alternatively, one might neglect heat conduction along those streams experiencing slug flows. However, the high thermal conductivities of liquid metal fuels and coolants make this a poor assumption in any reactor region of reasonably compact geometry.

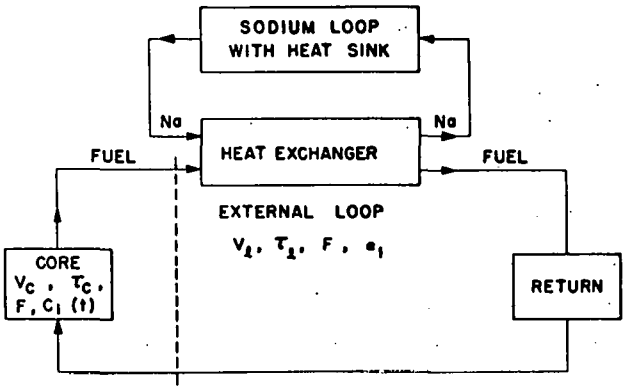

Fig. 3. Model for analysis of circulating-fuel reactor.

$\tau_c = V_c/F$ = core transit time

$\tau_\ell = V_\ell/F$ = external loop transit time

$C_i(t)$ = concentration of ith precursor in core at time t

λ_i = decay constant of ith precursor

α_i = fraction of ith precursor escaping external extraction.

It should be noted here that a separate fuel pump and conventional (noncontacting) heat exchanger could be used in Fig. 3. In that case, the analysis presented in this report is still valid if $\alpha_i = 1$ is specified.

Under the conditions of Fig. 3, the modified reactor kinetic equations can be written as

$$\frac{dn}{dt} = \frac{\rho - \beta}{\Lambda} n + \sum_i \lambda_i C_i(t), \tag{1}$$

$$\frac{dC_i}{dt} = \frac{\beta_i}{\Lambda} n - \lambda_i C_i(t) - \frac{C_i(t)}{\tau_c} + \frac{C_i(t - \tau_\ell)\, e^{-\tau_\ell \lambda_i}\, \alpha_i}{\tau_c} \tag{2}$$

where

$n = n(t)$ = neutron concentration in core

ρ = reactivity

Λ = generation time

β_i = fractional precursor yield

β = total precursor yield

Equation 1 is the usual core neutron density equation, while the terms of Eq. 2 represent the core precursor balance, namely,

$$\left|\begin{matrix}\text{rate of}\\ \text{change of}\\ \text{precursors}\end{matrix}\right| = \left|\begin{matrix}\text{rate of}\\ \text{formation}\end{matrix}\right| - \left|\begin{matrix}\text{rate of}\\ \text{decay in}\\ \text{core}\end{matrix}\right| - \left|\begin{matrix}\text{rate of}\\ \text{removal}\\ \text{from core}\end{matrix}\right| + \left|\begin{matrix}\text{rate of}\\ \text{return}\\ \text{to core}\end{matrix}\right| .$$

Equations 1 and 2 will be linearized by use of the assumptions

$$\begin{aligned} n(t) &= n_o + \Delta n(t) \\ \rho(t) &= \rho_o + \Delta\rho(t) \\ C_i(t) &= C_{io} + \Delta C_i(t) \\ C_i(t - \tau_\ell) &= C_{io} + \Delta C_i(t - \tau_\ell). \end{aligned} \tag{3}$$

The steady state value of n_o is arbitrary, but it is necessary to determine the steady state values of C_i and ρ. For the steady state, Eq. 2 becomes

$$0 = \frac{\beta_i}{\Lambda} n_o - C_{io}\left(\lambda_i + \frac{1}{\tau_c} - \frac{\alpha_i\, e^{-\tau_\ell \lambda_i}}{\tau_c}\right).$$

Rearrangement gives

$$C_{io} = \frac{n_o}{\Lambda}\frac{\beta_i}{\lambda_i}\left(\frac{\lambda_i}{\lambda_i + \frac{1}{\tau_c} - \frac{\alpha_i\, e^{-\tau \lambda_i}}{\tau_c}}\right) = \frac{n_o}{\Lambda}\frac{\beta_i\, a_i}{\lambda_i}, \tag{4}$$

where

$$a_i = \frac{\lambda_i}{\lambda_i + \frac{1}{\tau_c} - \frac{\alpha_i}{\tau_c} e^{-\tau \lambda_i}} .$$

Equation 4 states that the decay of precursors in the core, $\lambda_i C_{io}$, is less than their rate of production, $\beta_i n_o/\Lambda$, by the group effectiveness factor, a_i, which allows for precursor decay and extraction outside the core.

Similarly, for the steady state, Eq. 2 becomes

$$0 = (\rho_o - \beta)\frac{n_o}{\Lambda} + \sum \lambda_i C_{io} . \tag{5}$$

With Eq. 4, the summation becomes

$$\sum \lambda_i C_{io} = \frac{n_o}{\Lambda} \sum_i \beta_i a_i = \frac{n_o}{\Lambda} \beta a ,$$

where

$$a = \frac{\sum_i \beta_i a_i}{\beta} .$$

Substituting this result into Eq. 5, we obtain

$$\rho_o = (1 - a)\beta \ . \tag{6}$$

Equation 6 indicates that the steady state reactivity, ρ_o, is not zero unless the overall effectiveness factor, a, is unity -- as it is for a noncirculating-fuel reactor. In the limit, as a approaches zero, the steady state reactivity approaches β, corresponding to one dollar of reactivity and criticality on prompt neutrons alone.

It is now possible to determine the linearized kinetic equations. Substituting assumptions 3 into Eq. 1 gives

$$\frac{d\Delta n(t)}{dt} = [\rho_o - \Delta\rho(t) - \beta]\frac{[n_o + \Delta n(t)]}{\Lambda} + \sum_i \lambda_i [C_{io} + \Delta C_i(t)] .$$

Neglecting the products of small variations, using steady state Eq. 5 and the value of ρ_o from Eq. 6, we obtain

$$\frac{d\Delta n(t)}{dt} = \frac{n_o}{\Lambda}\Delta\rho(t) - \frac{a\beta}{\Lambda}\Delta n(t) + \sum_i \lambda_i \Delta C_i(t). \tag{7}$$

The linearized precursor equation is obtained similarly from Eq. 2:

$$\frac{d\Delta C_i(t)}{dt} = \frac{\beta_i}{\Lambda}\Delta n(t) - \frac{\lambda_i \tau_c + 1}{\tau_c}\Delta C_i(t) + \frac{\alpha_i e^{-\tau_\ell \lambda_i}}{\tau_c} C_i(t - \tau_\ell). \tag{8}$$

Equations 1, 2, 4, 6, 7, and 8 are in exact agreement with Eqs. 1, 2, 11, 12, 13, and 14 of Ref. 3, allowing for our extensions of the problem and for differences in notation.

In the matter of notation, however, there is more than a superficial difference. We have written the basic kinetics equations rigorously in terms of reactivity, ρ, and generation time, Λ. In Ref. 3, excess k, δk, and prompt neutron lifetime, ℓ, are used, but certain simplifying approximations are made in writing the kinetics equations which result in an exact correspondence with our rigorous equations based on ρ and Λ.

Lewins[4] gives a lucid exposition of the use of generation time, the reciprocal production probability, in reactor kinetics. The resulting equations are always simpler to solve than are those based on lifetime, the reciprocal destruction probability. For that large class of reactors for which Λ tends to be more nearly constant than does ℓ, the equations based on generation time are also more accurate.

We now investigate the response to a sinusoidal driving reactivity function specified by

$$\Delta\rho(t) = \overline{\Delta\rho}\, e^{j\omega t} = \overline{\Delta\rho}\, e^{st} \tag{9}$$

where $\overline{\Delta\rho}$ is the amplitude and $s = j\omega$. Other variables respond at the same frequency, and at amplitudes (denoted by bars) which are in general complex, that is, they include a phase shift. These are

$$\overline{\Delta n}(t) = \overline{\Delta n}\, e^{j\omega t} = \overline{\Delta n}\, e^{st}$$

$$C_i(t) = \overline{\Delta C_i}\, e^{j\omega t} = \overline{\Delta C_i}\, e^{st}$$

$$\Delta C_i(t - \tau_\ell) = C_i\, e^{j\omega(t-\tau_\ell)} = \Delta C_i\, e^{-s\tau_\ell}\, e^{st} \tag{10}$$

Substituting assumptions 9 and 10 into Eq. 7 and cancelling the factor e^{st} common to all terms yields

$$s\overline{\Delta n} = \frac{n_o}{\Lambda}\overline{\Delta\rho} - \frac{a\beta}{\Lambda}\overline{\Delta n} + \sum_i \lambda_i \overline{\Delta C_i} \ .$$

Rearrangement gives

$$\frac{\overline{\Delta n}}{n_o}(\Lambda s + a\beta) = \overline{\Delta\rho} + \frac{\Lambda}{n_o}\sum_i \lambda_i \overline{\Delta C_i} \ . \tag{11}$$

Similarly, Eq. 8 gives

$$s\,\overline{\Delta C_i} = \frac{\beta_i}{\Lambda}\overline{\Delta n} - \frac{\lambda_i \tau_c + 1}{\tau_c}\overline{\Delta C_i} + \frac{\alpha_i e^{-\tau_\ell \lambda_i}}{\tau_c}\overline{\Delta C_i}\, e^{-\tau_\ell s},$$

$$\frac{\beta_i}{\Lambda}\overline{\Delta n} = \left[s + \lambda_i + \frac{1}{\tau_c} - \frac{\alpha_i}{\tau_c} e^{-\tau_\ell(s+\lambda_i)}\right]\overline{\Delta C_i}$$

$$= (s + \lambda_i^*)\,\overline{\Delta C_i},$$

where

$$\lambda_i^* = \lambda_i + \frac{1}{\tau_c} - \frac{\alpha_i}{\tau_c} \exp[-\tau_\ell(s + \lambda_i)].$$

The resulting value

$$\overline{\Delta C_i} = \frac{\beta_i}{s + \lambda_i} \frac{\overline{\Delta n}}{\Lambda}$$

is used in Eq. 11 to obtain

$$\frac{\Delta n}{n_o}\left(\lambda s + a\beta - \sum \frac{\lambda_i \beta_i}{s + \lambda_i^*}\right) = \Delta\rho.$$

The zero-power transfer function can now be written

$$G(s) = \frac{\overline{\Delta n/n_o}}{\overline{\Delta\rho/\beta}} = \frac{\beta}{\Lambda s + a - \sum_i \frac{\lambda_i \beta_i}{s + \lambda_i^*}}$$

$$G(\omega) = \frac{\beta}{j\omega\Lambda + a\beta - \sum_i \frac{\lambda_i \beta_i}{j\omega + \lambda_i^*}} . \qquad (12)$$

If $\Sigma a_i\beta_i$ is substituted for $a\beta$, Eq. 12 can be expanded to

$$G(\omega) = \frac{\beta}{j\omega\Lambda + \sum_i a_i\beta_i\left(\frac{j\omega + \lambda_i^* - \frac{\lambda_i}{a_i}}{j\omega + \lambda_i^*}\right)} .$$

We can rewrite λ_i^* as

$$\lambda_i^* = \lambda_i + \frac{1}{\tau_c} - \frac{\alpha_i}{\tau_c} \exp(-\tau_\ell\lambda_i) \cos \omega\tau_\ell + j\frac{\alpha_i}{\tau_c} \exp(-\tau_\ell\lambda_i) \sin \omega\tau_\ell,$$

and, from the definition of a_i, we can write

$$\frac{\lambda_i}{a_i} = \lambda_i + \frac{1}{\tau_c} - \frac{\lambda_i}{\tau_c} \exp(-\tau_\ell\lambda_i).$$

Using these results, we obtain

$$G(\omega) = \frac{\beta}{j\omega\Lambda + \sum_i (a_i\beta_i) \frac{\left[\frac{\alpha_i}{\tau_c} e^{-\tau_\ell\lambda_i} (1 - \cos \omega\tau_\ell)\right] + j\left(\omega + \frac{\alpha_i}{\tau_c} e^{-\tau_\ell\lambda_i} \sin \omega\tau_\ell\right)}{\left(\lambda_i + \frac{1}{\tau_c} - \frac{\alpha_i}{\tau_c} e^{-\tau_\ell\lambda_i} \cos \omega\tau_\ell\right) + j\left(\omega + \frac{\alpha_i}{\tau_c} e^{-\tau_\ell\lambda_i} \sin \omega\tau_\ell\right)}} \qquad (13)$$

$$= \frac{\beta}{j\omega\Lambda + \sum_i (a_i\beta_i) \frac{Z_i + j\,Y_i}{X_i + j\,Y_i}} , \qquad (14)$$

where the definitions of X_i, Y_i, and Z_i are apparent. Further manipulation yields

$$G(\omega) = \frac{\beta}{\left[\sum_i (a_i\beta_i) \frac{X_i Z_i + Y_i^2}{X_i^2 + Y_i^2}\right] + j\left[\omega\Lambda + \sum_i (a_i\beta_i) \frac{X_i Y_i - Y_i Z_i}{X_i^2 + Y_i^2}\right]} = \frac{\beta}{R + jQ} , \qquad (15)$$

the definitions of R and Q being apparent. An alternative form for Eq. 15 is

$$G(\omega) = \frac{R - jQ}{R^2 + Q^2} . \qquad (16)$$

Finally, we find

$$\text{amplitude} = \frac{\beta}{R^2 + Q^2}\sqrt{R^2 + Q^2} = \frac{\beta}{\sqrt{R^2 + Q^2}} ,$$

$$\text{amplitude in decibels} = 20 \log_{10} \frac{\beta}{\sqrt{R^2 + Q^2}}$$

$$\tan \theta = -\frac{Q}{R} .$$

The above equations for the zero-power transfer function were coded for the IBM 704, and two check-out cases were run: one from Ref. 3 (τ_c = 0.96, τ_ℓ = 11.52) for circulating-fuel reactors, and one

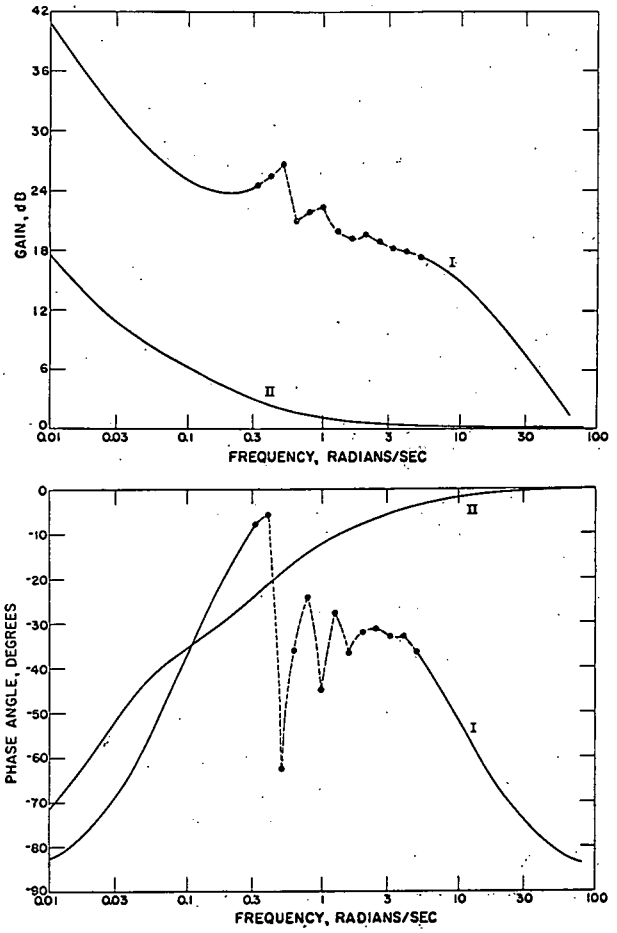

Fig. 4. Zero-power transfer function for two check cases: I = MacPhee;[3] II = LAMPRE.[5]

for the LAMPRE I reactor.[5] The results, shown in Fig. 4, agree well with those of the original authors. Note that MacPhee's definition of $G(\omega)$ is larger than ours by a factor β^{-1}. Hence, his gains are displaced upward by $20 \log_{10}(0.0074)^{-1} = 42.6$ dB.

The low-frequency behavior may be discussed by referring to Eq. 13. At low frequencies, if $\omega \ll 1/\tau_\ell$,

$$X_i \simeq \lambda_i + \frac{1}{\tau_c} - \frac{\alpha_i}{\tau_c} e^{-\tau_\ell \lambda_i} = \frac{\lambda_i}{a_j} ,$$

$$Y_i \simeq \omega\left(1 + \alpha_i \frac{\tau_\ell}{\tau_c} e^{-\tau_\ell \lambda_i}\right) ,$$

$$Z_i \simeq 0 .$$

Equation 15 then becomes

$$G(\omega) \simeq \frac{\beta}{\left[\sum_i (a_i\beta_i) \frac{Y_i^2}{X_i^2 + Y_i^2}\right] + j\left[\omega\Lambda + \sum_i (a_i\beta_i) \frac{X_iY_i}{X_i^2 + Y_i^2}\right]} .$$

Further, if ω is so small that $Y_i \ll X_i$, and if $\omega \ll 1/\tau_\ell$ and $\omega \ll \lambda_i/a_i$, we have in Eqs. 15 and 16

$$R \simeq 0 ,$$

$$Q \simeq \omega\left[\Lambda + \sum_i (a_i\beta_i) \frac{Y_i/\omega}{X_i}\right] ,$$

$$Q' = \frac{Q}{\omega} \simeq \Lambda + \sum_i \frac{a_i^2 \beta_i}{\lambda_i}\left(1 + \alpha_i \frac{\tau_\ell}{\tau_c} e^{-\tau_\ell \lambda_i}\right) .$$

Finally, at these low frequencies, Eq. 16 becomes

$$G(\omega) \simeq -j \frac{\beta}{Q} = -j \frac{\beta/Q'}{\omega} = -j \frac{\omega_1}{\omega} ,$$

where the constant ω_1, the low break frequency, is

$$\omega_1 = \frac{\beta}{\Lambda + \sum_i \frac{a_i^2 \beta_i}{\lambda_i}\left(1 + \alpha_i \frac{\tau_\ell}{\tau_c} e^{-\tau_\ell \lambda_i}\right)} .$$

In practice, the generation time Λ is so small (10^{-3} to 10^{-8} sec) as to be negligible in this expression. In this study, the values of ω_1 ranged from about 0.1 to 1 rad/sec. On the other hand, Λ is of utmost importance at very high frequencies, where Eq. 12 becomes

$$G(\omega) \simeq \frac{\beta}{j\omega\Lambda} \simeq -j \frac{(\beta/\Lambda)}{\omega} , \qquad \text{if } \omega \gg \frac{a\beta}{\Lambda} .$$

The high break frequency, $\omega_2 = \frac{\beta}{\Lambda}$, varies from about 10 rad/sec for a typical thermal reactor to about 10^5 rad/sec for a typical fast reactor.

At intermediate frequencies, Eq. 12 reduces to

$$G(\omega) \simeq \frac{\beta}{a\beta} \simeq \frac{1}{a} , \qquad \text{if } \lambda_i \ll \omega \ll \frac{a\beta}{\Lambda} .$$

Approximate limits for typical thermal and fast reactors are, respectively, $3 \ll \omega \ll 10$ and $3 \ll \omega \ll 10^5$. Thus, a broad plateau with gain $1/a$ exists for fast reactors, whereas only a narrow one, if any, is present in thermal reactors.

The resonance behavior may be seen by examining Eqs. 13 and 14. The quantities X_i and Z_i exhibit

undamped oscillations, repeating as ω changes by

$$\Delta\omega = \frac{2\pi}{\tau_\ell}$$

The quantity Y_i is essentially proportional to ω, but with superimposed oscillations of the above periodicity $\Delta\omega$ and of constant amplitude. These oscillations become less important relative to ω as ω increases.

Resonances are most likely to occur when $\alpha = 1$, that is, when none of the neutron precursors are extracted in the external loop. Therefore, for this case, a parametric study was made for various values of loop time. The results shown in Fig. 5 indicate that some peaking occurs at long loop times, but that all peaking dies away as the loop time decreases. The values $\tau_c = 0.67$ and $\tau_\ell = 0.5$ are typical of the higher-powered reactors to be considered. No significant peaking is found for these values.

Figures 6-8 show results for various combinations of τ_c, τ_ℓ, and α. No resonances are indicated by any of the graphs.

POWER FEEDBACK TRANSFER FUNCTION

When a reactor operates at substantial powers, a reactivity feedback loop comes into play through the fuel's temperature coefficient of reactivity. In order to determine the reactivity feedback, it is first necessary to determine the relationship between change in power and change in fuel temperature. A power-temperature transfer function may be defined, for small sinusoidal variations at the frequency ω, as

$$H(\omega) = \frac{\overline{\Delta T_o}}{\overline{\Delta P}} , \qquad (17)$$

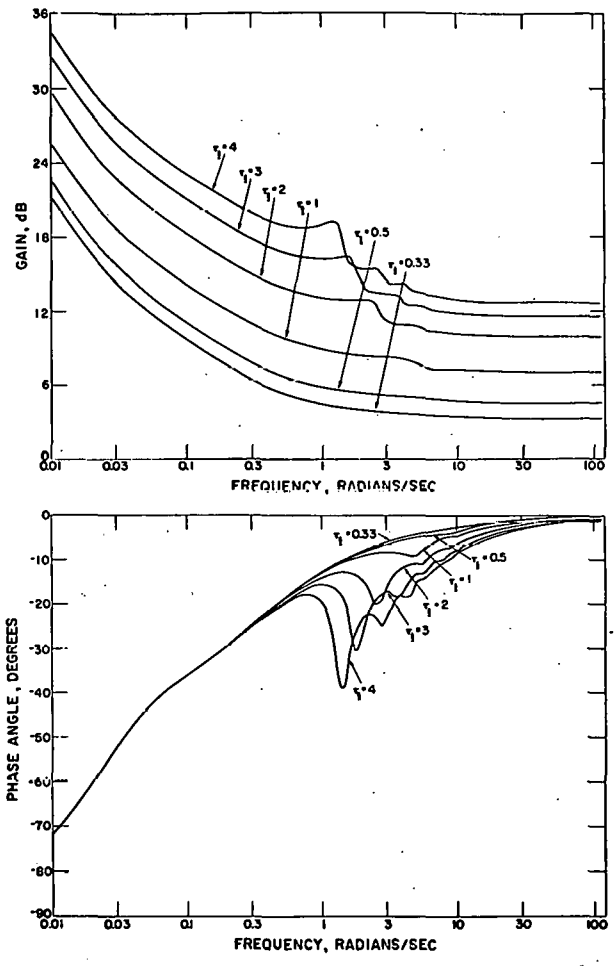

Fig. 5. Zero-power transfer functions for $\alpha_i = 1$ (no precursor extraction) and $\tau_c = 0.67$ sec; τ_ℓ as parameter.

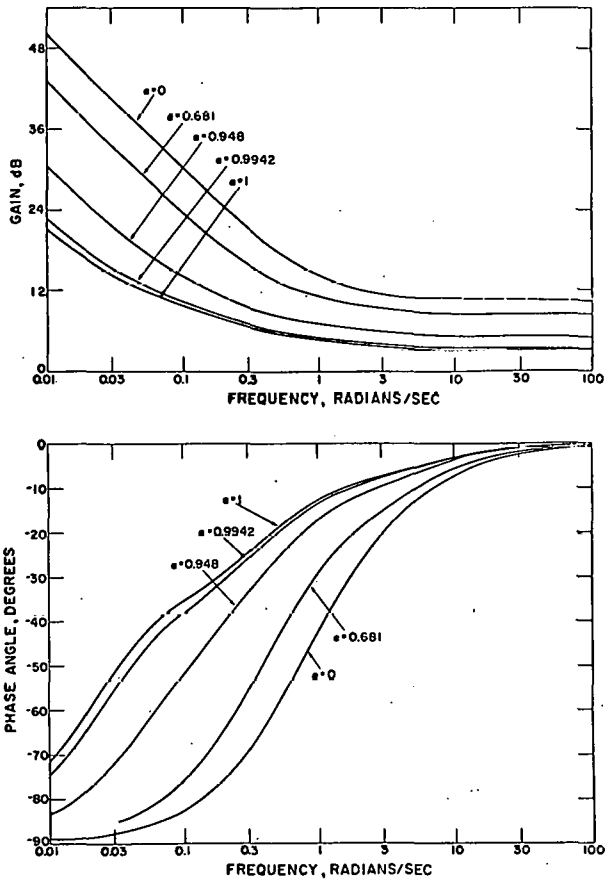

Fig. 6. Zero-power transfer functions for $\tau_c = 2.0$ sec and $\tau_\ell = 1.0$ sec; α_i as parameter.

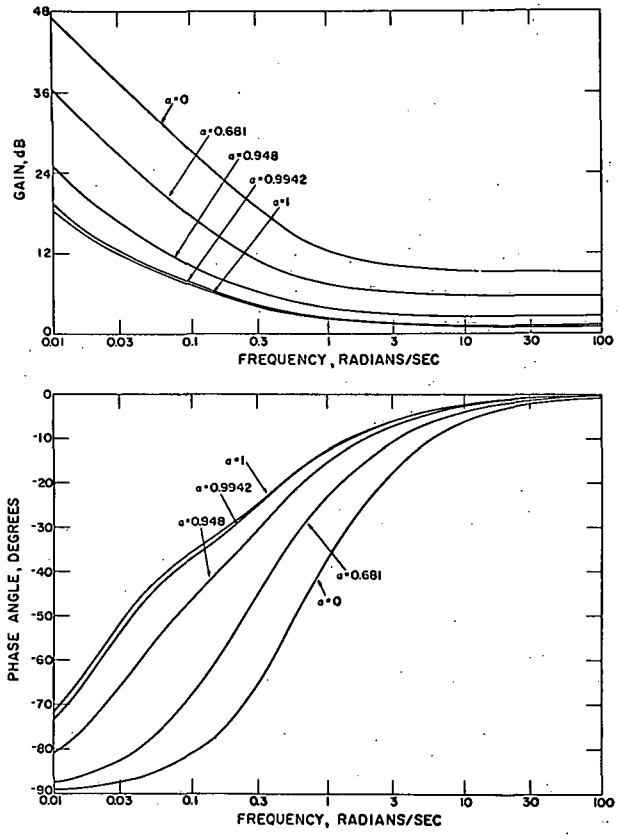

Fig. 7. Zero-power transfer functions for τ_c = 2.67 sec and τ_ℓ = 0.33 sec; α_i as parameter.

where $\overline{\Delta T}_o$ is the change in average fuel temperature resulting from the change in power, $\overline{\Delta P}$. Again, the bars denote complex amplitudes, including phase shifts.

The closed loop feedback system is shown schematically in Fig. 9, where $\overline{\Delta\rho}_t$ is the reactivity change caused by the temperature change $\overline{\Delta T}_o$ through the fuel temperature coefficient of reactivity $\partial\rho/\partial T_o$.

The relationship between neutron density and power,

$$\frac{\overline{\Delta P}}{P_o} = \frac{\overline{\Delta n}}{n_o} ,$$

can be used in Eq. 17 to obtain

$$\overline{\Delta T}_o = H(\omega)\ P_o\ \frac{\overline{\Delta n}}{n_o} .$$

This result may be used in connection with Fig. 9 to give

$$\frac{\Delta\rho_t}{\beta} = \frac{1}{\beta}\frac{\partial\rho}{\partial T_o} H(\omega)\ P_o\ \frac{\overline{\Delta n}}{n_o} = -H'(\omega)\ \frac{\overline{\Delta n}}{n_o} , \qquad (18)$$

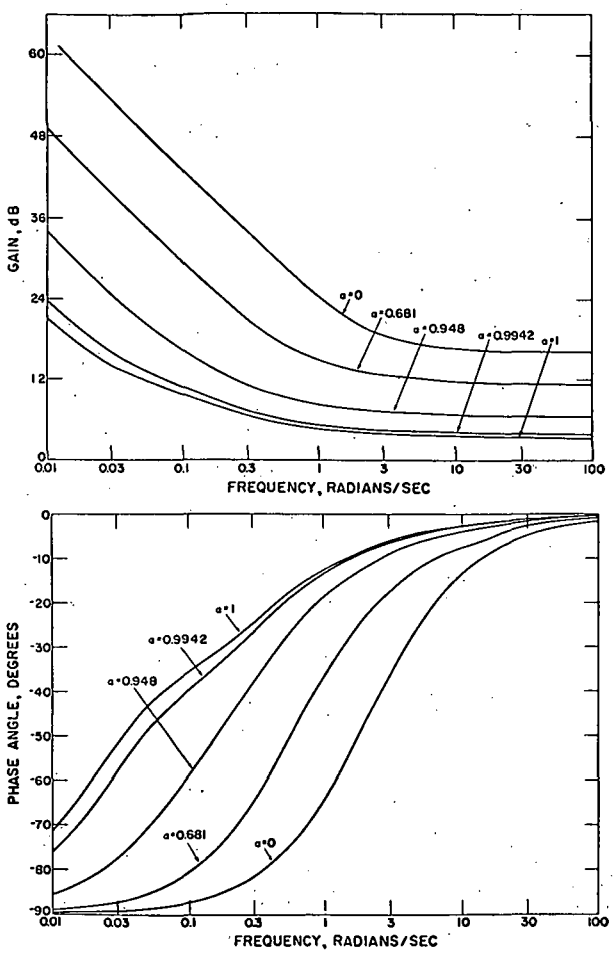

Fig. 8. Zero-power transfer functions for τ_c = 0.67 sec and τ_ℓ = 0.33 sec; α_i as parameter.

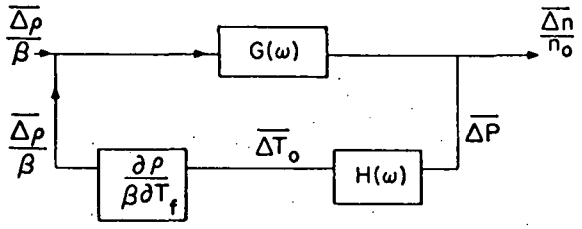

Fig. 9. Closed loop feedback system.

where

$$H'(\omega) = -\frac{1}{\beta}\frac{\partial\rho}{\partial T_o} H(\omega)\ P_o .$$

We can define the total reactor transfer function as

$$R(\omega) = \frac{\overline{\Delta n}/n_o}{\overline{\Delta\rho}/\beta} . \qquad (19)$$

It can be seen from Fig. 9 that

$$\frac{\overline{\Delta n}}{n_o} = G(\omega)\left(\frac{\Delta\rho}{\beta} + \frac{\Delta\rho_t}{\beta}\right) .$$

Combining this result with Eqs. 18 and 19 yields

$$R(\omega) = \frac{G(\omega)}{1 + G(\omega)\, H'(\omega)} .$$

The next step is to determine $H'(\omega)$. The power equation in the core is

Heat generated = heat raising core temperature

+ net heat carried out by flow,

$$P = \rho_f\, C_f\left[V_c\, \frac{dT_o}{dt} + F(T_o - T_i)\right] , \quad (20)$$

where

ρ_f = fuel density

C_f = fuel specific heat

T_i = fuel temperature at core inlet

T_o = fuel temperature at core outlet and (assuming instantaneous mixing) in the core.

Let the sinusoidal driving reactivity 9 result in

$$\begin{aligned} P &= P_o + \overline{\Delta P} e^{j\omega t} \\ T_i &= T_{io} + \overline{\Delta T}_i e^{j\omega t} \\ T_o &= T_{oo} + \overline{\Delta T}_o e^{j\omega t} . \end{aligned} \quad (21)$$

Substitution of Eq. 21 into Eq. 20 gives

$$P_o + \overline{\Delta P} e^{j\omega t} = \rho_f\, C_f\left[V_c\, j\omega\, \Delta T_o + F(\overline{\Delta T}_o - \overline{\Delta T}_i)\right] e^{j\omega t} + \rho_f\, C_f\, F(T_{oo} + T_{io}) . \quad (22)$$

When the initial condition,

$$P_o = \rho_f\, C_f\, F(T_{oo} - T_{io}),$$

is subtracted from Eq. 22 and the result divided by $e^{j\omega t}$, we get

$$\overline{\Delta P} = \rho_f\, C_f\left[V_c\, j\omega\, \overline{\Delta T}_o + F(\overline{\Delta T}_o - \overline{\Delta T}_i)\right] . \quad (23)$$

The fuel circuit is divided into three parts: core, heat exchanger, and return, as in Fig. 10. The following additional quantities are now introduced:

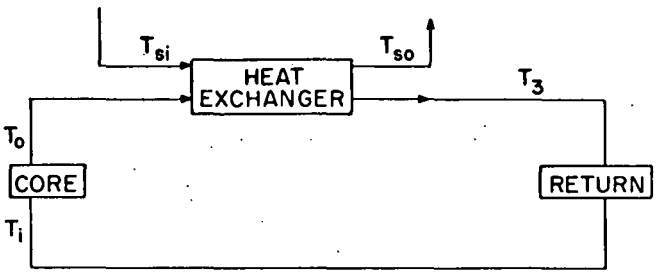

Fig. 10. Fuel and coolant temperature schematic.

T_3 = temperature of fuel in heat exchanger

$\gamma = \rho_f\, C_f\, F$

$C_c = \rho_f\, C_f\, V_c$

$C_r = \rho_f\, C_f\, V_r$

$C_{hx} = \rho_f\, C_f\, V_{hx}$

V_{hx} = volume of fuel in the heat exchanger

V_r = volume of fuel in return

T_{so} = temperature of sodium in heat exchanger

K = heat transfer coefficient of the heat exchanger

Then Eq. 23 becomes

$$\overline{\Delta P} = (\gamma + j\omega\, C_c)\, \overline{\Delta T}_o - \gamma \overline{\Delta T}_i . \quad (24)$$

Assuming the fuel to be isothermal in the return at temperature T_i, the heat balance is

$$F\rho_f\, C_f(T_3 - T_i) = \frac{dT_i}{dt}\, \rho_f\, C_f\, V_r ,$$

and the variations become

$$\gamma(\overline{\Delta T}_3 - \overline{\Delta T}_i) = j\omega\, \overline{\Delta T}_i\, C_r . \quad (25)$$

The heat balance for the fuel in the heat exchanger, assuming the fuel to be isothermal there at temperature T_3, is

$$K(T_3 - T_{so}) = F\rho_f\, C_f(T_o - T_3) - \frac{dT_3}{dt}\, \rho_f\, C_f\, V_{hx} \quad (26)$$

The heat balance in the sodium coolant of the heat exchanger, assuming an isothermal sodium temperature T_{so}, is

$$K(T_3 - T_{so}) = C_s\, \rho_s\, V_s\, \frac{dT_{so}}{dt} + F_s\, \rho_s\, C_s(T_{so} - T_{si}) \quad (27)$$

where

C_s = specific heat of sodium in the heat exchanger

ρ_s = density of sodium in the heat exchanger

V_s = volume of sodium in the heat exchanger

F_s = volumetric flow of sodium through the heat exchanger

T_{si} = sodium inlet temperature to the heat exchanger (assumed constant)

When perturbed, Eqs. 26 and 27 can be expressed as

$$K(\overline{\Delta T}_3 - \overline{\Delta T}_{so}) = \gamma(\overline{\Delta T}_o - \overline{\Delta T}_3) - j\omega\, \Delta T_3\, C_{hx} \tag{28}$$

and

$$K(\overline{\Delta T}_3 - \overline{\Delta T}_{so}) = C_{sx}\, j\omega\, \overline{\Delta T}_{so} + \gamma_s\, \overline{\Delta T}_{so}, \tag{29}$$

where

$$C_{sx} = \rho_s\, C_s\, V_s\ ,$$

$$\gamma_s = \rho_s\, C_s\, F_s\ .$$

Rearrangement of Eq. 29 gives

$$\overline{\Delta T}_{so} = \frac{K}{K + \gamma_s + j\omega\, C_{sx}}\, \overline{\Delta T}_3\ . \tag{30}$$

Substitution of Eq. 30 into Eq. 28 yields

$$K\,\overline{\Delta T}_3 - \frac{K^2\,\overline{\Delta T}_3}{K + \gamma_s + j\omega\, C_{sx}} = \gamma\overline{\Delta T}_o - \gamma\overline{\Delta T}_3 - j\omega\, C_{hx}\,\overline{\Delta T}_3$$

from which

$$\overline{\Delta T}_3 = \frac{\gamma}{K - \dfrac{K^2}{K + \gamma_s + j\omega\, C_{sx}} + \gamma + j\omega\, C_{hx}}\, \overline{\Delta T}_o\ . \tag{31}$$

Substituting Eq. 31 into Eq. 25 gives

$$\overline{\Delta T}_i = \frac{\gamma}{\gamma + j\omega\, C_r}\, \overline{\Delta T}_3$$

$$= \frac{\gamma^2}{(\gamma + j\omega\, C_r)\left(\dfrac{K(\gamma_s + j\omega\, C_{sx})}{K + \gamma_s + j\omega\, C_{sx}} + \gamma + j\omega\, C_{hx}\right)}\, \overline{\Delta T}_o\ . \tag{32}$$

Using Eq. 32 in Eq. 24, we obtain $\overline{\Delta P}$ in terms of $\overline{\Delta T}_o$ and use this in Eq. 17 to obtain

$$H(\omega) = \left[(\gamma + j\omega\, C_c) - \frac{\gamma^2}{(\gamma + j\omega\, C_r)\left(\dfrac{\gamma_s + j\omega\, C_{sx}}{1 + \dfrac{1}{K}(\gamma_s + j\omega\, C_{sx})} + \gamma + j\omega\, C_{hx}\right)}\right]^{-1}\ . \tag{33}$$

By straightforward manipulations of the complex expressions, Eq. 33 can be transformed into

$$H(\omega) = L + jM,$$

where L and M are lengthy combinations of the quantities appearing in Eq. 33. These have been incorporated into the FORTRAN code described below, but are not explicitly given here.

At low frequencies, Eq. 33 reduces to

$$H(\omega \to o) = \frac{1}{\gamma_s} + \frac{1}{K} + \frac{1}{\gamma} = \frac{1}{\rho_s\, C_s\, F_s} + \frac{1}{K} + \frac{1}{\rho_f\, C_f\, F}\ .$$

The three terms represent the temperature changes per unit power change (e.g., °C/W) contributed in the sodium stream, the heat exchange interface, and the fuel stream. These are additive, as one might expect, the sodium temperature T_{si} being the fixed point in temperature.

At high frequencies, Eq. 33 becomes

$$H(\omega \to \infty) = \frac{1}{j\omega\, C_c} = -j\left(\frac{1}{\rho_f\, C_f\, V_c}\right)\left(\frac{1}{\omega}\right)\ .$$

The factor $\rho_f\, C_f\, V_c$ represents a type of time constant (e.g., °C/W-sec) for the core.

The power coefficient of reactivity can be defined as

$$H_p(\omega) = -\frac{1}{\beta}\frac{\partial \rho}{\partial T_o}\,\frac{\overline{\Delta T}_o}{\overline{\Delta P}} = -\frac{1}{\beta}\frac{\partial \rho}{\partial T_o}\, H(\omega),$$

with units, for example, of \$/W. Thus, the results given above can be used to obtain the low frequency power coefficient (approaching the steady state coefficient as the frequency approaches zero) and the high frequcncy power coefficient.

It is seen that $H(\omega)$ depends only on thermal properties and parameters, and not at all on transit times or the precursor effectiveness factors. It will be shown below that at low frequencies $H'(\omega)$ dominates the reactor transfer function, so that the low frequency behavior is independent of transit time and precursor effectiveness.

TOTAL REACTOR TRANSFER FUNCTION

As shown previously, the total reactor transfer function depends upon both the zero-power transfer function and the power feedback function. The results obtained above are summarized as follows:

$$\left.\begin{aligned} R(\omega) &= \frac{G(\omega)}{1 + G(\omega)\, H'(\omega)} \quad , \\ G(\omega) &= \frac{\beta(R + jQ)}{R^2 + Q^2} \quad , \\ H'(\omega) &= \frac{1}{\beta}\left(\frac{\partial \rho}{\partial T_o}\right) H(\omega)\, P_o \quad , \\ H(\omega) &= L + jM \quad . \end{aligned}\right\} \tag{34}$$

The quantities appearing in these equations were determined in the previous section in terms of basic reactor parameters. By complex-number manipulations, $R(\omega)$ can be transformed into

$$\left.\begin{aligned} R(\omega) &= S + jT \quad , \\ \text{phase} &= \arctan \frac{T}{S} \quad , \\ \text{amplitude} &= \sqrt{S^2 + T^2} . \end{aligned}\right\} \tag{35}$$

Expressions for S and T, in terms of the quantities in Eqs. 34, were incorporated into the code described below. This result appears to be a consequence of the isothermal conditions of Assumption (vi) stated in the Introduction. Had we, alternatively, neglected heat conduction along the fuel stream, it seems likely that transit time dependence, including resonant effects, would have resulted.

EXAMPLES

The results of MacPhee for one delayed neutron group at zero power had indicated some peaking when certain core and loop times were considered.[3] It was thus of interest to determine whether this occurred for core and loop times comparable to those of the Fast Reactor Core Test Facility (FRCTF) and also to determine the effect of neutron precursor extraction in the external loop. The delayed neutron parameters of Table I, corresponding to fast fission in ^{239}Pu, were chosen. These parameters are taken from Ref. 6, for $\nu = 3.000$ neutrons per fission. The values for the percent of delayed neutron precursors extracted were taken from the work of R. M. Bidwell.[2]

TABLE I

DELAYED NEUTRON PARAMETERS

$\beta_1 = 7.98 \times 10^{-5}$	$\lambda_1 = 1.29 \times 10^{-2}$
$\beta_1^1 = 5.88 \times 10^{-4}$	$\lambda_1^1 = 3.11 \times 10^{-2}$
$\beta_3^2 = 4.536 \times 10^{-4}$	$\lambda_3^2 = 1.34 \times 10^{-1}$
$\beta_4^3 = 6.888 \times 10^{-4}$	$\lambda_4^3 = 3.31 \times 10^{-1}$
$\beta_5^4 = 2.163 \times 10^{-4}$	$\lambda_5^4 = 1.26 \times 10^{0}$
$\beta_6^5 = 7.350 \times 10^{-5}$	$\lambda_6^5 = 3.21 \times 10^{0}$

Three reactors were chosen for extensive transfer function analysis. A schematic representation of the lift-pump version for FRCTF is shown in Fig. 2, and the constants are listed in Table II (2.5-MW and 15-MW reactors). The 287-MW reactor, for which the constants are given in Table II, is similar to that of Ref. 1.

Some calculational results for these three reactor systems are shown graphically in Figs. 11-13.

DISCUSSION OF RESULTS

Instability in a reactor system may be indicated by the occurrence of a resonance in the transfer function at one or more values of input frequency. In this study, resonances occur only in the graphs of some zero-power transfer functions $G(\omega)$ for unrealistic systems having long loop times. For the three reactor systems studied, such resonances did not occur.

The function $H'(\omega)$ appears to be entirely free of resonances.* At low frequencies, it approaches a real constant (proportional to the steady-state power coefficient) similar to that for noncirculating fuel systems. As the frequency increases, the imaginary component becomes dominant. Curves for $H'(\omega)$ are given only for the nominal power in each system, since $H'(\omega)$ is simply proportional to power.

At low frequencies, the total reactor transfer function $R(\omega)$ of Eqs. 34 is the reciprocal of $H'(\omega)$, because the product $G(\omega)\, H'(\omega)$ dominates the denominator at these frequencies. As the frequency increases, the $H'(\omega)$ function decreases so that, at high frequencies, the denominator approaches unity and $R(\omega)$ approaches $G(\omega)$.

*See footnote at the end of the section on Power Feedback Transfer Function for an explanation.

TABLE II

CONSTANTS FOR THREE REACTORS

Constant	Units	2.5-MW Reactor	15-MW Reactor	287-MW Reactor
Core flow rate, F	(m^3/sec)	4.826×10^{-3}	2.896×10^{-2}	0.4
Volume of core, V_c	(m^3)	2.574×10^{-2}	2.574×10^{-2}	0.224
Fuel density, ρ_f	(kg/m^3)	8650	8650	7500
Specific heat of fuel, C_f	(MW-sec/kg-°C)	2.3926×10^{-4}	2.3926×10^{-4}	2.65×10^{-4}
Fuel volume in pool, V_r	(m^3)	5.4×10^{-3}	5.4×10^{-3}	0.15
Fuel volume in mixed flow, V_{hx}	(m^3)	7.542×10^{-3}	7.542×10^{-3}	0.07
Heat transfer coefficient, K	(MW/°C)	4×10^{8}	4×10^{8}	10^{10}
Specific heat of sodium, C_s	(MW-sec/kg-°C)	1.2555×10^{3}	1.2555×10^{3}	1.2555×10^{3}
Density of sodium, ρ_s	(kg/m^3)	780	780	780
Volume of sodium in mixed flow, V_s	(m^3)	2.263×10^{-2}	2.263×10^{-2}	0.210
Sodium flow rate, F_s	(m^3/sec)	1.448×10^{-2}	8.688×10^{-2}	1.2
Reactivity temperature coefficient, $\frac{\partial \rho}{\partial T_o}$	$(°C^{-1})$	-6×10^{-5}	-6×10^{-5}	-6×10^{-5}
Time in core, τ_c	(sec)	5.3328	0.8888	0.56
Time in external loop, τ_ℓ	(sec)	2.6664	0.444	0.55
Fraction of precursors not extracted, α_i		0.948[a]	0.948[a]	0.681[b]
Precursor effectiveness factor, a (based on above input)		0.686	0.506	0.227

[a] lift pump

[b] jet pump

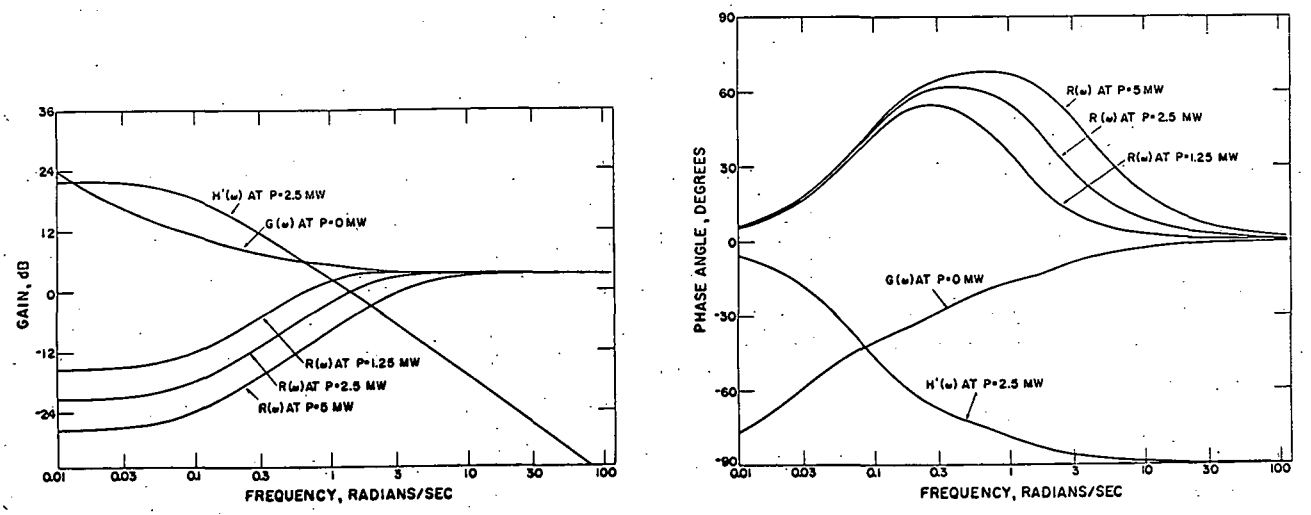

Fig. 11. Transfer functions for the 2.5-MW reactor.

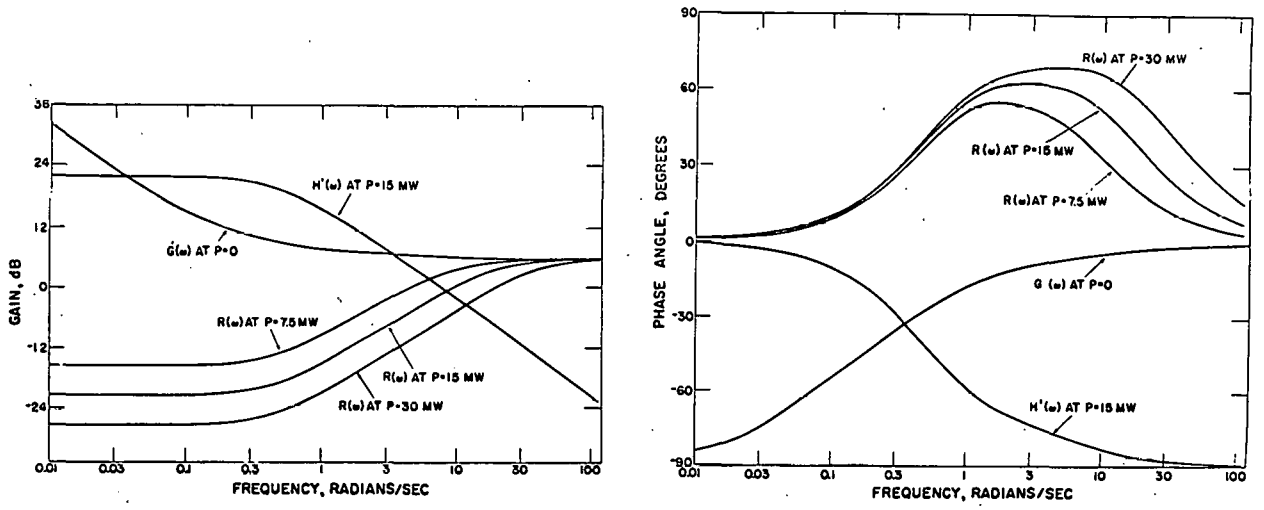

Fig. 12. Transfer functions for the 15-MW reactor.

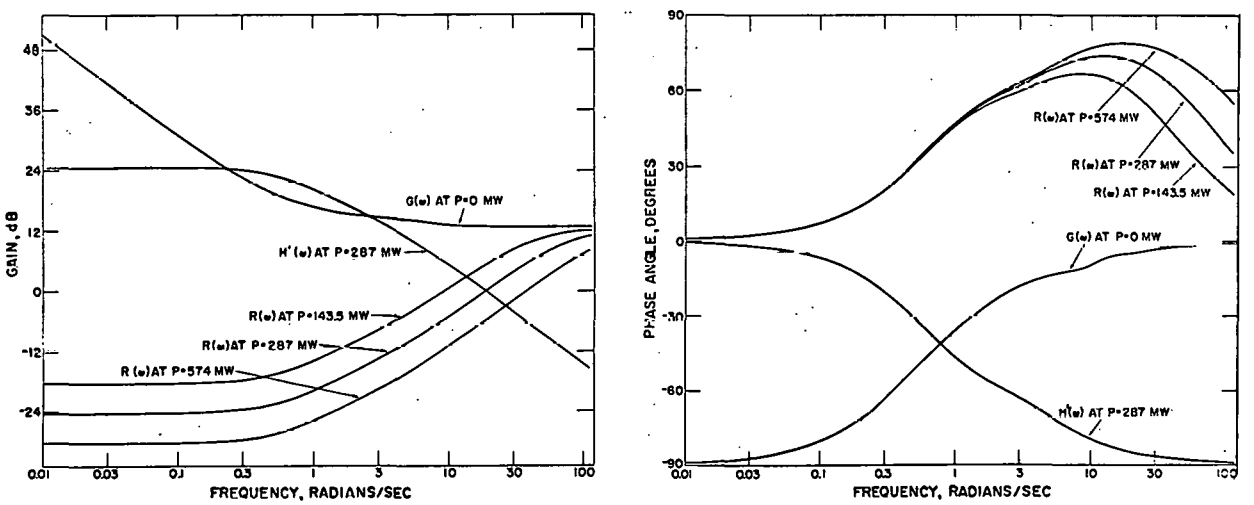

Fig. 13. Transfer functions for the 287-MW reactor.

At intermediate frequencies, the phase angle of $R(\omega)$ is a rather sensitive function of frequency, because $G(\omega)$ is almost completely real in this region, and $H'(\omega)$ is almost completely imaginary. Thus, the product $|G(\omega)|H'(\omega)$ is the tangent of the phase angle. The quantity $G(\omega)$ varies slowly, but $H'(\omega)$ varies rapidly in this region, so that the angle is also a rapidly varying function.

At frequencies in the range of possible resonances of $G(\omega)$, the total reactor transfer function is dependent on both $G(\omega)$ and $H(\omega)$, with the effect of $H(\omega)$ tending to be more important in the cases studied. Since $H(\omega)$ does not display the resonances sometimes seen in $G(\omega)$, the operation tends to be more stable at significant power than at zero power.

ACKNOWLEDGMENTS

The valuable assistance of B. M. Carmichael through helpful discussions and suggestions is gratefully acknowledged. Much credit is due C. R. DePoorter for her work in editing and organizing the material. Most of the work reported here was performed during the summer of 1961, when one of us (B.J.H.) was participating in the Summer Graduate Student Employment Program of the Los Alamos Scientific Laboratory.

REFERENCES

1. R. P. Hammond and J. R. Humphreys, Jr., Nucl. Sci. Eng. 18, 421 (1964).
2. R. M. Bidwell, Nucl. Sci. Eng. 18, 426 and 435 (1964).
3. J. MacPhee, Nucl. Sci. Eng. 4, 588 (1958).
4. J. Lewins, Nucl. Sci. Eng. 7, 122 (1960).
5. "LAMPRE I Final Design Status Report," LA-2833, p. 44 (March 1963).
6. G. Keepin, T. Wimett, and R. Ziegler, Phys. Rev. 107, 1044 (1957).